Global Sustainability Research
https://doi.org/10.56556/gssr.v2i3.515
ISSN: 2833-986X

RESEARCH ARTICLE

Spatial analysis of flash flood and drought impact from climate change in Phongsaly district, Phongsaly province, by using Geo-Informatics technology and Modelling

Sanxay Boutsamaly[1], Chankhachone Sonemanivong[2], Soulyphan Kannitha[2], Phoummixay Siharath[1]*, Somchay Vilaychaleun[1], Khampasith Thammathevo[1], Amphayvanh Oudomdeth[3], Tavanh Kittiphone[3]

[1]Environmental Engineering Department, Faculty of Engineering, National University of Laos
[2]Civil Engineering Department, Faculty of Engineering, National University of Laos
[3]Department of Climate Change, Ministry of Natural Resources and Environment

Corresponding Author: Sanxay Boutsamaly : J3ew.bsml@gmail.com
Received: 28 May, 2023, Accepted: 16 June, 2023, Published: 22 June, 2023

Abstract

A method for predicting the water resource in the region in the future to be used as a basis for mitigating the consequences is to study how climate change affects hydrology. The purpose of this study is to i). choose a global climate model that is suitable for the area, ii). rainfall run-off modelling, iii). drought and flood hazard index map. The SSP-126, SSP-245, and SSP-585 scenarios were chosen as the most appropriate global climate model among the four institutes, with efficiency criteria using the coefficient of Nash-Sutcliffe and Kling-Gupta and then calibrate the data with the Bias Correction Linear Scaling method which divides the analysis period into 2 periods for Near-Future and Far-Future from analyzing Rainfall Run-off Modeling from Rainfall Concentration 1-hours, 3-hours and 6-hours. It was found that the SSP-585 scenario in the Rainfall Concentration 1-hours model has the most dangerous area for very high risk until the end of the 21st century. For the analysis of drought indices SPI_1, SPI_3 and SPI_6 in Near-Future, it was found that the frequency of droughts is increasing according to the worst scenario, the scenario with the most drought is SSP-585 and in the Far-Future, the frequency of drought is decreasing according to the worst scenario, the scenario with the most drought is SSP-126.

Keywords: Drought; Flood; Flash flood; Model; Climate change; IPCC

Introduction

In late 2021, the IPCC released its Sixth Assessment Report (AR6), detailing the rise in global temperatures to 1.5℃ Inevitably above pre-industrial levels, Floods and landslides are quite likely across Asia, and the continent's temperatures will rise. by proposing a new method for projecting greenhouse gases by bringing Shared Socioeconomic Pathway (SSP) applying a prediction to the end of the 21st century in 5 scenarios: (IPCC, Climate Change 2021: The Physical Science Basis, the Working Group I contribution to the Sixth Assessment Report, 2021).

- SSP1-1.9: A 1.5 °C temperature rise by 2050.
- SSP1-2.6: A 1.8 °C temperature rise by 2100.
- SSP2-4.5: A 2.7 °C temperature rise by 2100.
- SSP3-7.0: A 3.6 °C temperature rise by 2100.
- SSP5-8.5: A 4.4 °C temperature rise by 2100.

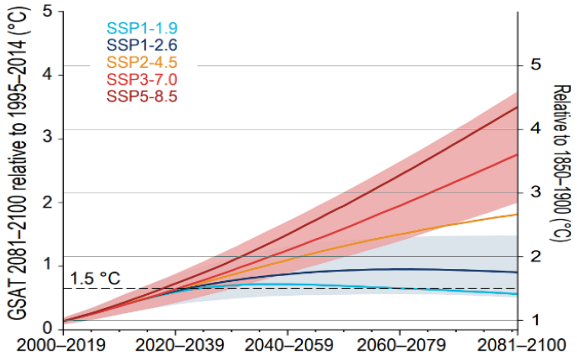

Figure 1. The graph shows the temperature increase in each scenario.

According to the Lao Green Climate Fund (GCF) Work Plan, Lao PDR has emitted 52,790Gg CO2eq of greenhouse gases into the atmosphere, of which 82% of total emissions come from land use change. In addition, after 2009, Lao PDR is prone to floods and droughts,

especially in the northern region, which often experiences flash floods. (GCF, 2021)

Lao PDR is a landlocked country. but has much more natural resources than many Asian nations, particularly in the areas of water, forests, and minerals. In 1940, the Lao PDR had 70% of its land covered in forests, but by 2002, that number had decreased to 41.5% (UNDP, 2012), making Lao PDR the 42nd most vulnerable country to climate change.

One of these is Phongsaly Province in the north of Lao PDR, which regularly experiences flash floods and droughts. Lao PDR is thought to be the country most susceptible to drought. because rivers and streams are where most people reside. The primary industry is agriculture. (ADB, 2012)

According to the Mekong River Commission's (MRC) Measuring Station's observational monitoring data for the years 2020–2022, the Phongsaly District experienced 40 droughts in total, including 9 severe, 5 extreme, and 1 catastrophic drought, the most of which took place between the July to December. (MRC, 2019)

Additionally, one of the Sustainable Development Goals (SDGs), the 13th goal with a plan to address it, includes addressing climate change (Climate Action).

In the scenario, it serves as a guideline for planning, mitigating, and adapting to climate change, as well as for resolving issues and creating a development plan for the Lao PDR to lessen the effects of potential disasters like floods and droughts brought on by the worsening severity of climate change. Additionally, it tries to adjust development strategies in accordance with the scenario and increase awareness of the severity of the issue. Therefore, we are interested in using geographic information systems and models to analyze the places in Phongsaly District and Phongsaly Province that have experienced floods and droughts because of climate change.

Literature review

Several studies have looked at global climate change issues, but in Lao PDR, there are still few regional studies. Phrakonkham, Khasama, et al. (2020), integrated and mapped hazards using the Analytical Hierarchy Process (AHP) across Laos. From the results of the study, it was found that hazard areas are distributed in the northern and southern regions of Lao PDR. Rasanak, Sanxay et al. (2021) studied the impact of climate change by using the CMIP5 global climate model and rainfall runoff model to map flood hazard areas in the Xedon basin in the southern part of Lao PDR. From the results, the most high-hazard area found in the far future, the RCP8.5 scenario, covers an area of 483.9 km2. Maisor et al. (2022) used the CMIP6 global climate model by making a flood hazard map in the Xechamphone Basin in the central region of Lao PDR. From the results of the study, it was found that in the near future, the SSP126 scenario has the most area of very high hazard, and in the near future, the SSP585 scenario has the most area of very high hazard. from earlier studies Natural disasters and climate change continue to have an adverse impact on many regions. There is still no regional climate change analysis in the northern part of Lao PDR, which is essential for planning mitigation strategies.

Methodology

Study area

The capital of Phongsaly Province, Phongsaly District, has a total area of 2,855 km2 and is located at latitude and longitude 208962 and 2419580, respectively, between (Zone) UTM 47 and 48N. It has a main river named Nam Ou and is the highest city in the Lao PDR; its northern border is with China, its southern border is with Xay District in Oudomxay Province, and its eastern border is with Thailand. Additionally, Phongsaly District has a favorable climate for agriculture and produces agricultural goods.

Phongsaly District, Phongsaly Province, is reportedly one of the regions that has suffered disasters every year for the previous ten years or more, according to reports from various organizations. together with the issue of climate change that the world is currently facing. As a result, we decided to research this issue's consequences to develop guidelines for avoiding and lessening its negative effects.

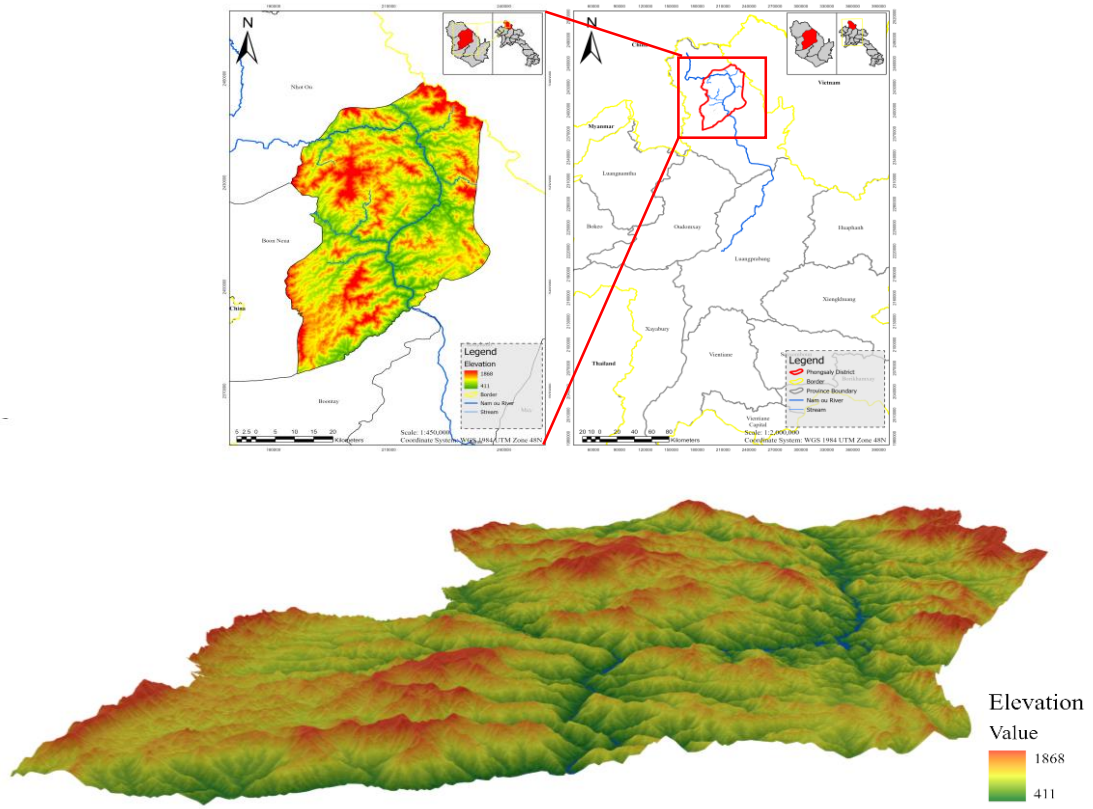

Figure 2. Map showing study area, elevation, and topography of Phongsaly Province.

For this study, we divided the analysis period into two time periods: the near future from 2018 to 2050 and the far future from 2051 to 2100, and daily rainfall data for a 21-year period (1997-2017) was collected from four stations in the Nam Ou catchment area, namely Phongsaly, Muong Ngoy, Dien Bien and Oudomxay. Refer to the data from the Mekong River Commission (MRC) rain gauge stations as shown in the table below. This historical data will be interpolated in an area with a resolution of 12.5 x 12.5 m by using the Inverse Distance Weight (IDW) technique. Global climate models by using downscaling techniques and adjusting data predictions to be as close to reality as possible. The most appropriate Global climate models were then selected for use in the analytical study.

Table 1. Rain gauge station used in this study.

No	Rain Gauge Station	Station ID	Time Intervals	Coordinate (UTM)		Source
				X	Y	
1	Phongsaly	210201	1922-2019	210505	2406007	Mekong River Commission (MRC)
2	Dien Bien	210301	1979-2022	293236	2363995	
3	Muong Ngoy	200201	1996-2017	259051	2290796	
4	Oudomxay	200204	1984-2019	810792	2289916	

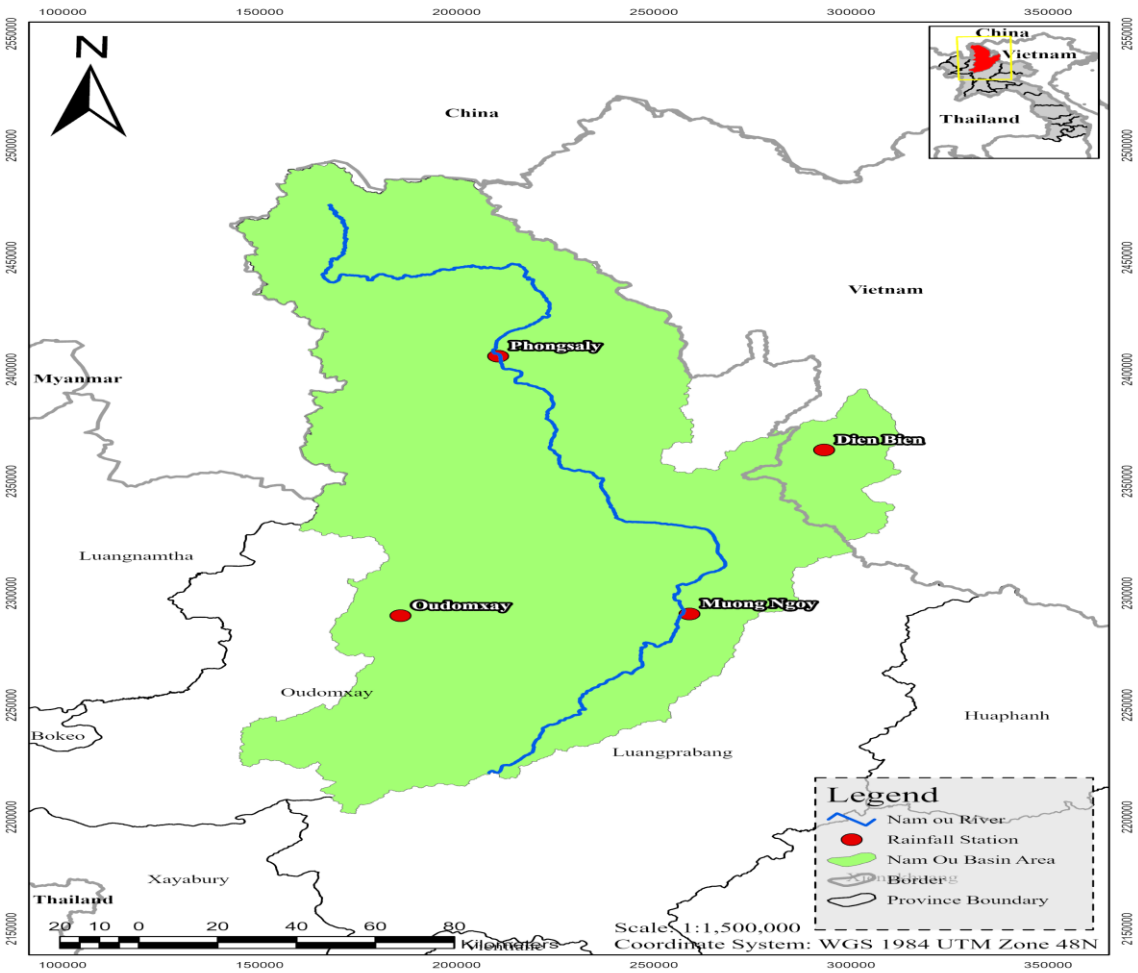

Figure 3. Map showing location of rain gauge station.

For simulated data collection, we rely on global climate models (GCMs) from four institutes. The 4 models are: the Institute Pierre Simon Laplace, France (IPSL), the Max Planck Institute for Meteorology, Germany (MPI), the Meteorological Institute, Norway (NorESM), the National Institute for Environmental Studies, and the Japan Agency for Marine-Earth Science and Technology, Japan (MIROC). which has forecast the rainfall data from now until the end of the 21st century, which is detailed in the table below:

Table 2. Global Climate Models are used in this study.

No	GCMs	Institute	Frequency	Resolution
1	IPSL-CM6A-LR	Institute Pierre Simon Laplace, France	day	2.5˚x 1.3˚
2	MPI-ESM1-2-LR	Max Planck Institute for Meteorology, Germany	day	1.9˚x 1.9˚
3	NorESM2-LM	Meteorological Institute, Norway	day	2.5˚x 1.9˚
4	MIROC6	National Institute for Environmental Studies, and Japan Agency for Marine-Earth Science and Technology, Japan	day	1.4˚x 1.4˚

Extract time series

The four institutes' climate models have different data sets. Therefore, we write a coding algorithm to retrieve data from specific global climate models using Python. So, we merged the files into one file first. and then retrieve information in the area we study.

Performance indicator

Nash-Sutcliffe efficiency (NSE)

Nash-Sutcliffe efficiency (NSE) (J.E. Nash, 1970) It is a popular index used to determine model accuracy or model performance. To estimate the desired value with the following formula:

$$\mathrm{NSE} = 1 - \frac{\sum_{i=1}^{n}(Y_i - \widehat{Y}_i)^2}{\sum_{i=1}^{n}(Y_i - \overline{Y})^2}$$

Where

Y_I: The observed value of I when I is between 1 and n.

$\widehat{Y}_I$: Prediction value Y_i

$\overline{Y}$: Mean value of Y_i

NSE have a value between -∞ to 1 Which can interpret the meaning of the NSE value as shown in the table below:

Table 3. Meaning of NSE value.

NSE Value	Model Accuracy
1	Perfect Fit
>0 - <1	Arithmetic Mean
0	The model can predict the values as accurately as the prediction using the mean.
<0	The model can predict with less accuracy than the mean estimate.
≥0.75	Good prediction (Yangqing Lian, 2007)
0.36 – 0.75	Satisfactory prediction (Yangqing Lian, 2007)

Kling-Gupta efficiency (KGE)

This measure of fit was created by (Hoshin V. Gupta, 2009) to aid Nash-Sutcliff performance categorization analysis. This makes it easier to evaluate the relative significance of the variables (correlation, bias, and variance) within the context of a hydrological model (Harald Kling, 2012), whose equations are as follows:

$$\mathrm{KGE} = 1 - \sqrt{(\mathrm{CC} - 1)^2 + (\frac{\mathrm{cd}}{\mathrm{rd}} - 1)^2 + (\frac{\mathrm{cm}}{\mathrm{rm}} - 1)^2}$$

Where

CC: Pearson Coefficient

rm: Average of Observed values

cm: Average of Forecast values

rd: Standard Deviation of Observation values

cd: Standard Deviation of Forecast values

The Pearson coefficient can be obtained from the equation below:

$$r = \frac{\sum_{i=1}^{n}(O_i - \overline{O})(P_i - \overline{P})}{\sqrt{\sum_{i=1}^{n}(O_i - \overline{O})^2}\sqrt{\sum_{i=1}^{n}(P_i - \overline{P})^2}}$$

Where

O_i: Observation value

P_i: Prediction value

$\overline{O}$: Mean value of O_i

$\overline{P}$: Mean value of P_i

Calibration

Large geographic resolution data are available from global climate models for precipitation forecasts. The data must be adjusted using Linear Scaling Bias Correction (LS) before using [9]. LS is a simple statistical estimating approach utilized in numerous investigations.

$$P_{his}(d)^* = P_{his}(d) \cdot [\mu_m\{P_{obs}(d)/\{\mu_m P_{his}(d)\}]$$

$$P_{sim}(d)^* = P_{sim}(d) \cdot [\mu_m\{P_{obs}(d)\}/\{\mu_m P_{his}(d)\}]$$

Where

P_{obs}: Observation data

P_{his}: Historical data from GCMs

P_{his}^*: Historical data from GCMs after Bias correction

P_{sim}^*: Precipitation data from GCMs after Bias correction

P_{sim}: Precipitation data from GCMs

d: Precipitation data

μ_m: Correction factor

Return period

To estimate the probabilities of total monthly rainfall and to estimate rainfall around the recurrence of total monthly rainfall in this research, we used a method (Weibull, 1939) to obtain a frequency of exceedance that is closest to the mean value of the distribution, with the following formula:

$$P = \frac{N}{(m+1)}$$

Where

P: Probability of exceedance

N: Total number of years record

m: Rank of observed rainfall value

T: Return period (mm) given by $T = \frac{1}{P}$

Standardized precipitation index (SPI)

(Thomas B. McKee, 1993) developed the SPI method to determine and monitor climate drought conditions, which is now used by various organizations. It is widely used to analyze the SPI index from monthly rainfall. The SPI will be analyzed over 3 periods, namely 1 month, 3 months, and 6 months, which this research will define as SPI_1, SPI_6, and SPI_12, respectively.

$$SPI = \frac{X_{ij} - X_{im}}{\sigma}$$

Where

X_{ij}: Precipitation for the station i month j (mm)

X_{im}: Mean precipitation (mm)

σ: Standardized deviation

The criteria used by the SPI to categorize drought levels are listed in the table below:

Table 4. Drought Classification based on SPI (McKee et al., 1993)

Drought classes	SPI
≥ 2	Extremely wet (EW)
1.50 to 1.99	Very wet (SW)
1.00 to 1.49	Moderately wet (MW)
-0.99 to 0.99	Near normal (N)
-1.00 to -1.49	Severely dry (MD)
-1.50 to -1.99	Severely dry (SD)
≤ -2	Extremely dry (ED)

Flood hazard index classification

By considering the flood depth of each square in the flood map and converting it to a value is a disaster index, we proposed the hazard level with a flood disaster index adjusted for the relationship between flood depth and velocity (Sally J. Priest, 2009), as shown in the table and figure below:

Table 5. Flood depth-hazard index relationship**.**

Flood depth (m)	Hazard index
Small hazard < 0.3	0.00 – 0.25
Medium hazard < 0.6	0.25 – 0.50
High risk < 2	0.50 – 0.75
Very high risk > 2	0.70 – 1.00

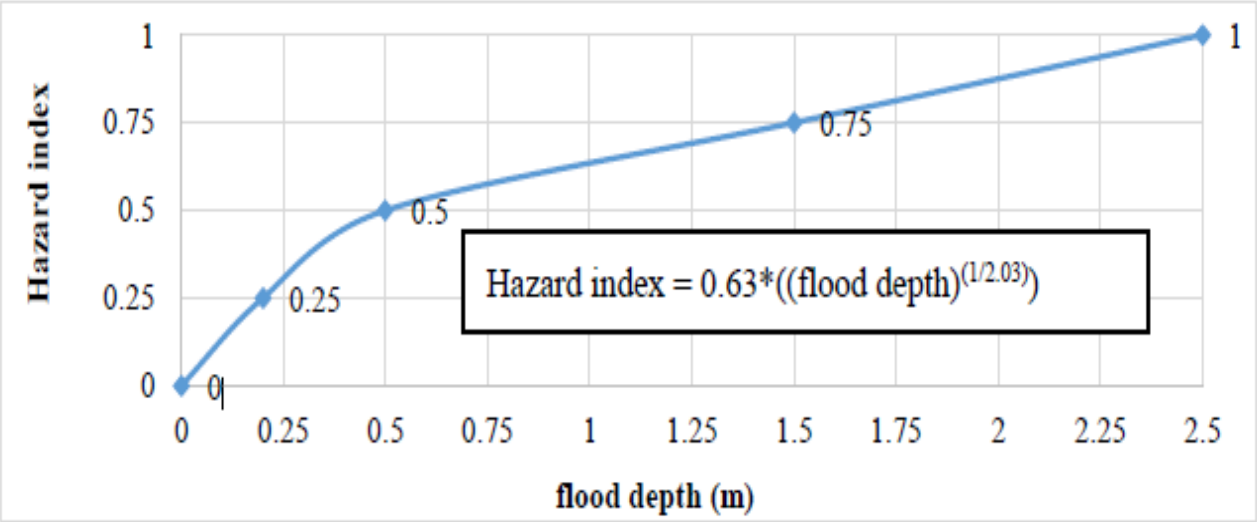

Figure 4. Flood depth and hazard index relationship curve.

Results and discussions

Performance indicator

Using observed rainfall data from five stations in the watershed area and historical data from four GCMs, a performance indicator was developed using Nash-Sutcliffe and Kling-Gupta. From the result of the distribution of monthly rainfall with observed and simulated data, in most cases the simulated data is much less than the actual observed data, but in most cases the sample is close to the actual rainfall data.

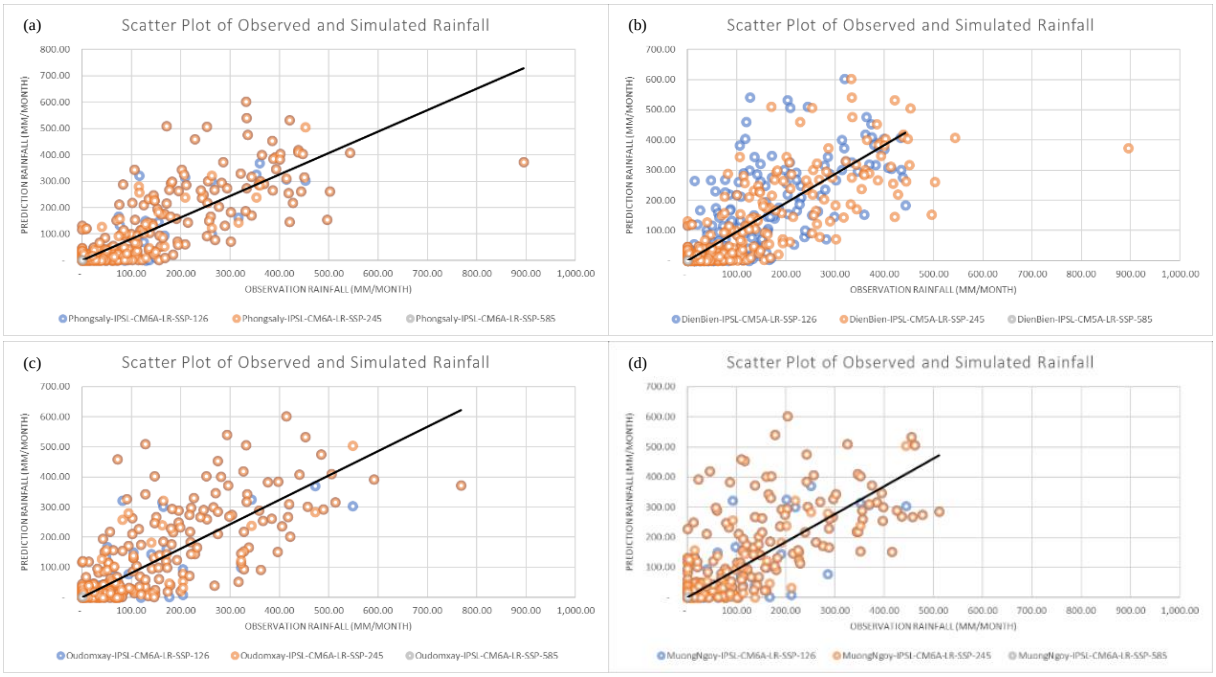

Figure 5. Scatter plot of observed and simulated data: (a) Phongsaly-IPSL-CM6A-LR, (b) DienBien-IPSL-CM6A-LR, (c) Oudomxay-IPSL-CM6A-LR and (d) MuongNgoy-IPSL-CM6A-LR.

The IPSL-CM6A-LR, which has an average coefficient primarily near 1, is the model that is most suitable according to Nash-Sutcliffe and Kling-Gupta performance indicator, which also places the MPI-ESM1-2-LR, MIROC6, and NorESM2-M next.

Table 6. Efficiency value of Nash-Sutcliffe and Kling-Gupta.

Nash-Sutcliffe Efficiency												
Rainfall Station	**Predicted Rainfall**											
	IPSL-CM6A-LR			**MIROC6**			**MPI-ESM1-2-LR**			**NorESM2-M**		
	SSP126	**SSP245**	**SSP585**	**SSP126**	**SSP245**	**SSP585**	**SSP126**	**SSP245**	**SSP585**	**SSP126**	**SSP245**	**SSP585**
Phongsaly	0.553	0.558	0.564	0.367	0.343	0.380	0.406	0.416	0.404	0.259	0.250	0.261
DienBien	0.552	0.552	0.554	0.379	0.354	0.381	0.605	0.630	0.624	0.293	0.285	0.281
Oudomxay	0.478	0.477	0.452	0.332	0.277	0.358	0.457	0.487	0.487	0.207	0.191	0.201
Muong Ngoy	0.493	0.513	0.527	0.361	0.324	0.375	0.627	0.646	0.642	0.203	0.194	0.189
Average scenario	**0.519**	**0.525**	**0.524**	**0.360**	**0.324**	**0.374**	**0.524**	**0.545**	**0.539**	**0.241**	**0.230**	**0.233**
Average GCMs	**0.52**			**0.35**			**0.54**			**0.23**		
Kling-Gupta Efficiency												
Rainfall Station	**Predicted Rainfall**											
	IPSL-CM6A-LR			**MIROC6**			**MPI-ESM1-2-LR**			**NorESM2-M**		
	SSP126	**SSP245**	**SSP585**	**SSP126**	**SSP245**	**SSP585**	**SSP126**	**SSP245**	**SSP585**	**SSP126**	**SSP245**	**SSP585**
Phongsaly	0.74	0.74	0.747	0.66	0.64	0.65	0.56	0.56	0.56	0.63	0.62	0.63
DienBien	0.65	0.65	0.65	0.58	0.57	0.58	0.66	0.69	0.68	0.49	0.48	0.48
Oudomxay	0.67	0.66	0.65	0.62	0.60	0.62	0.62	0.63	0.63	0.60	0.59	0.59
Muong Ngoy	0.63	0.64	0.65	0.59	0.57	0.59	0.66	0.66	0.66	0.50	0.50	0.50
Average Scenario	**0.675**	**0.674**	**0.673**	**0.61**	**0.59**	**0.61**	**0.62**	**0.63**	**0.63**	**0.55**	**0.55**	**0.55**
Average GCMs	0.67			0.60			0.63			0.55		
Average Efficiency	**0.60**			**0.48**			**0.58**			**0.39**		

Model calibration

The observed precipitation data over a 21-year period was used in a bias correction process with historical data from the IPSL-CM6A-LR based on scenarios SSP-126, SSP-245, and SSP-585. The analysis found that the historical data was lower than the observed rainfall. But in some scenarios, it's the opposite. which is shown in the cumulative distribution curve as follows:

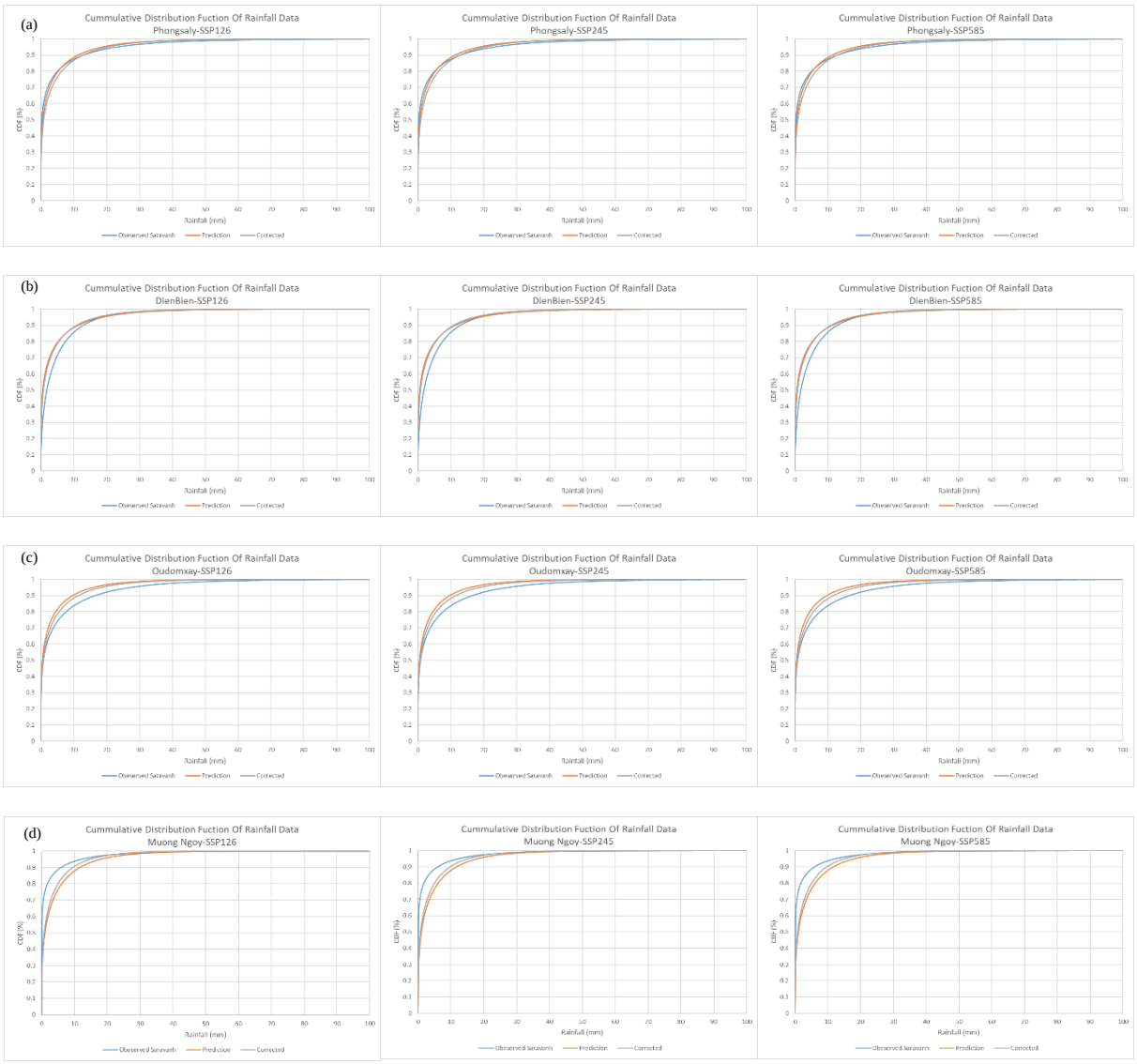

Figure 6. Cumulative distribution function of rainfall data at rainfall stations (a) Phongsaly, (b) DienBien, (c) Oudomxay, and (d) Muong Ngoy based on each scenario.

Flood hazard

1 Hour concentration interval

In the near future, the area prone to very high-risk flooding under the SSP-126 scenario is 87.13 km^2, the SSP-245 scenario has an area of 160.73 km^2, an increased from the SSP-126 scenario of 84.46%, and the SSP585 scenario has an area of 180.20 km^2, an increased from the scenario in SSP-245 by 12.11%. According to the analysis, the scenario at SSP-585 was the worst-case scenario.

In the far future, the area prone to very high-risk flooding under the SSP-126 scenario is 170.95 km2, the SSP-245 scenario has an area of 168.90 km2, a decreased from the SSP-126 scenario of -1.20%, and the SSP585 scenario has an area of 171.08 km2, an increased from the scenario in SSP-245 by 1.29%. According to the analysis, the scenario at SSP-585 was the worst-case scenario.

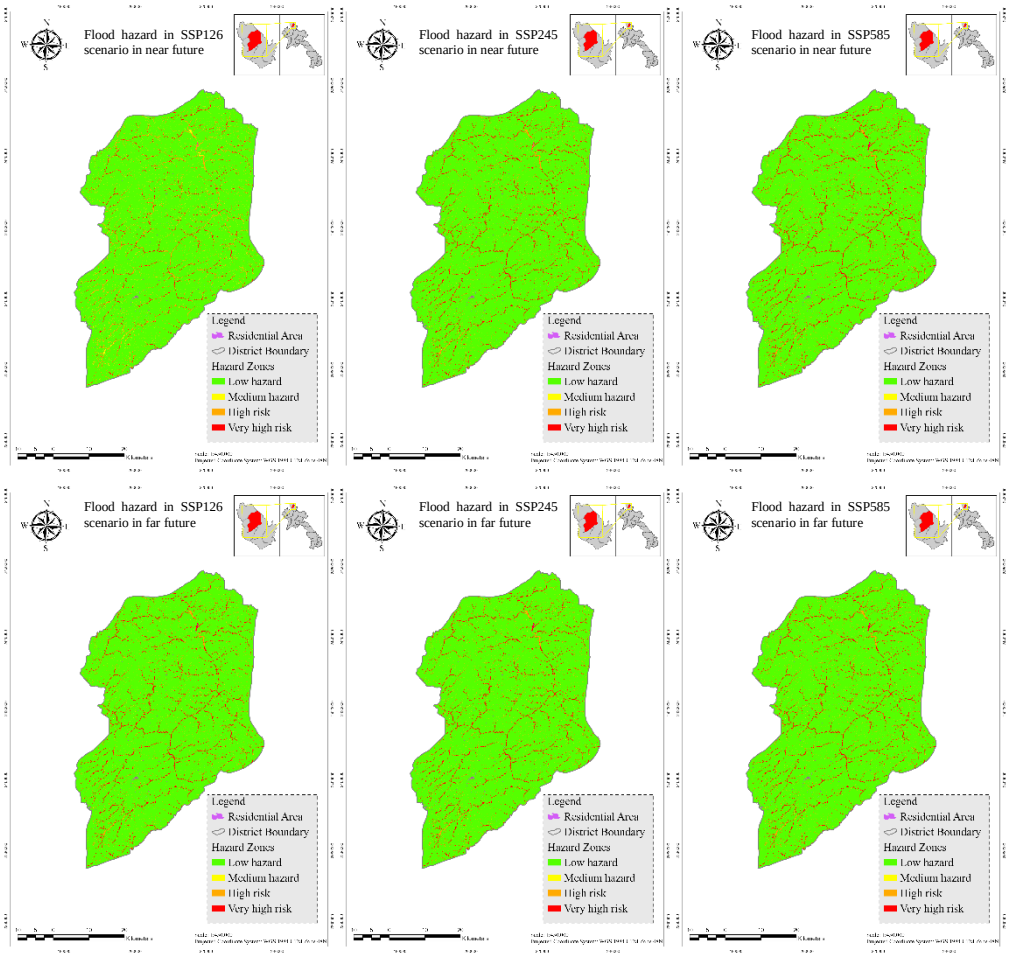

Figure 7. Flood hazard map in 1 hour's concentration of rainfall for each scenario.

Table 7. Flood hazard area in 1 hour's concentration of rainfall for each scenario.

1 Hours Concentration Interval Flood Hazard Area (km^2)							
No	**Hazard Zones**	**Near Future**			**Far Future**		
		SSP126	**SSP245**	**SSP585**	**SSP126**	**SSP245**	**SSP585**
1	Low hazard	2627.25	2630.79	2613.99	2622.64	2624.57	2622.53
2	Medium hazard	36.49	9.83	9.87	9.96	9.88	9.98
3	High risk	99.97	49.50	46.78	47.29	47.50	47.25
4	Very high risk	87.13	160.73	180.20	170.95	168.90	171.08

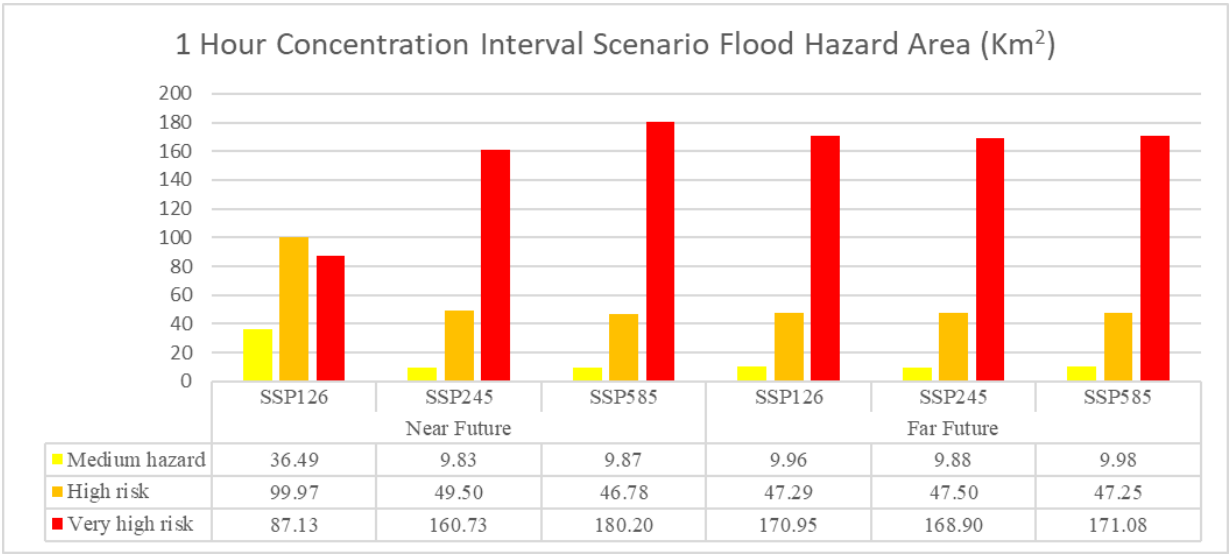

	SSP126	SSP245	SSP585	SSP126	SSP245	SSP585
	Near Future			Far Future		
Medium hazard	36.49	9.83	9.87	9.96	9.88	9.98
High risk	99.97	49.50	46.78	47.29	47.50	47.25
Very high risk	87.13	160.73	180.20	170.95	168.90	171.08

Figure 8. Graph showing comparison of the area in 1 hour's concentration of rainfall for each scenario.

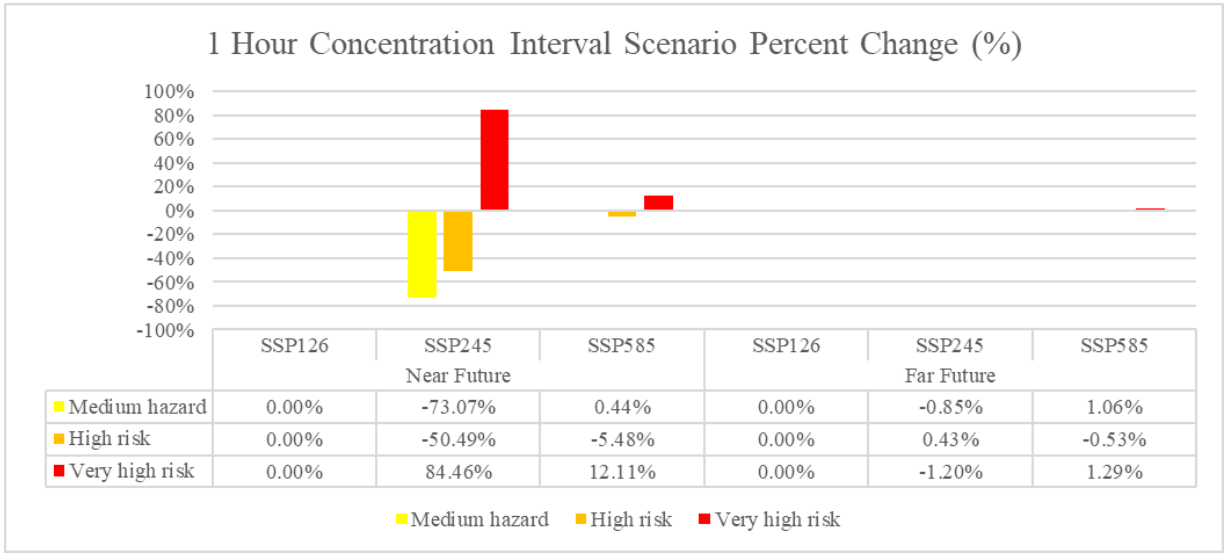

	SSP126	SSP245	SSP585	SSP126	SSP245	SSP585
	Near Future			Far Future		
Medium hazard	0.00%	-73.07%	0.44%	0.00%	-0.85%	1.06%
High risk	0.00%	-50.49%	-5.48%	0.00%	0.43%	-0.53%
Very high risk	0.00%	84.46%	12.11%	0.00%	-1.20%	1.29%

Figure 9. Graph showing the percent change in area in 1 hour's concentration of rainfall for each scenario.

3 Hour concentration interval

In the near future, the area prone to very high-risk flooding under the SSP-126 scenario is 160.69 km^2, the SSP-245 scenario has an area of 158.12 km^2, a decreased from the SSP-126 scenario of -1.60%, and the SSP585 scenario has an area of 170.01 km^2, an increased from the scenario in SSP-245 by 7.52%. According to the analysis, the scenario at SSP-585 was the worst-case scenario.

In the far future, the area prone to very high-risk flooding under the SSP-126 scenario is 165.70 km^2, the SSP-245 scenario has an area of 164.56 km^2, a decreased from the SSP-126 scenario of -0.69%, and the SSP585 scenario has an area of 165.74 km^2, an increased from the scenario in SSP-245 by 0.72%. According to the analysis, the scenario at SSP-585 was the worst-case scenario.

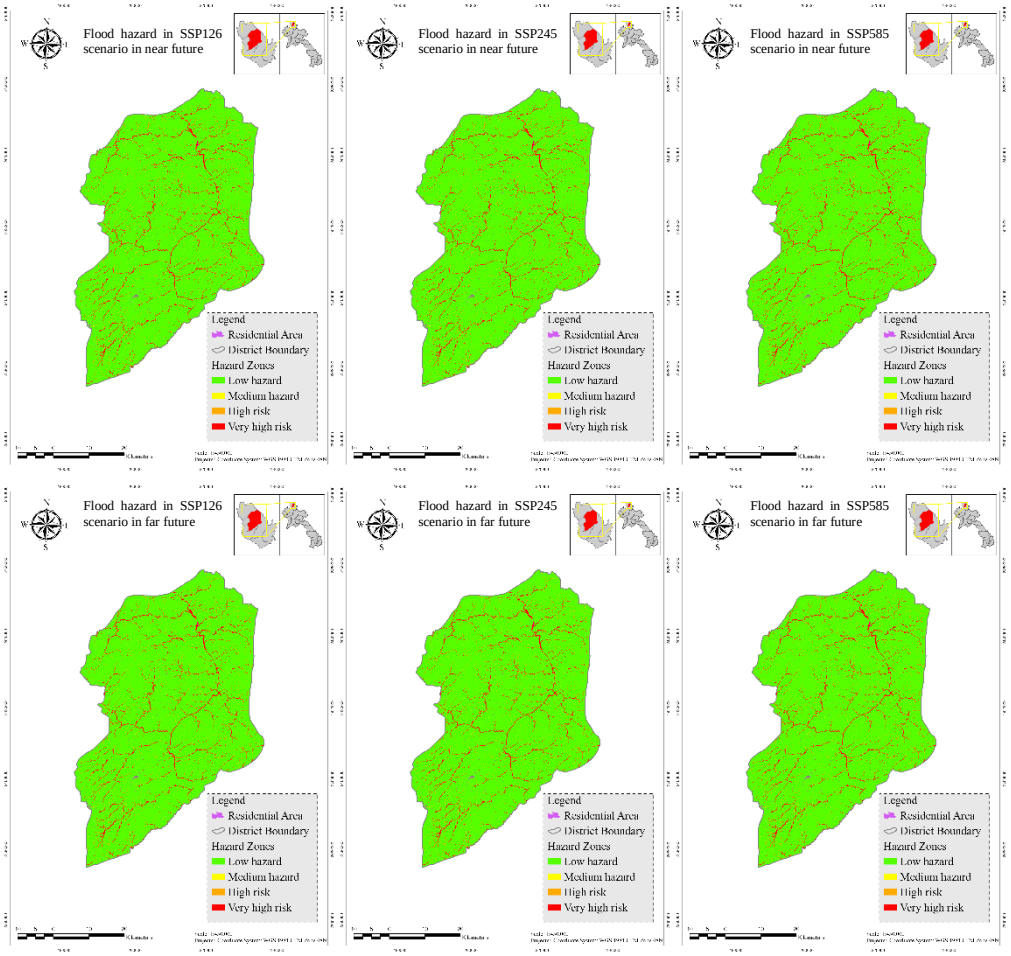

Figure 10. Flood hazard map in 3 hour's concentration of rainfall for each scenario.

Table 8. Flood hazard area in 3 hour's concentration of rainfall for each scenario.

3 Hours Concentration Interval Flood Hazard Area (km^2)

No	Hazard Zones	Near Future			Far Future		
		SSP126	SSP245	SSP585	SSP126	SSP245	SSP585
1	Low hazard	2640.82	2643.48	2631.20	2635.61	2636.78	2635.50
2	Medium hazard	9.35	9.36	9.29	9.27	9.37	9.30
3	High risk	39.98	39.89	40.35	40.26	40.13	40.29
4	Very high risk	160.69	158.12	170.01	165.70	164.56	165.74

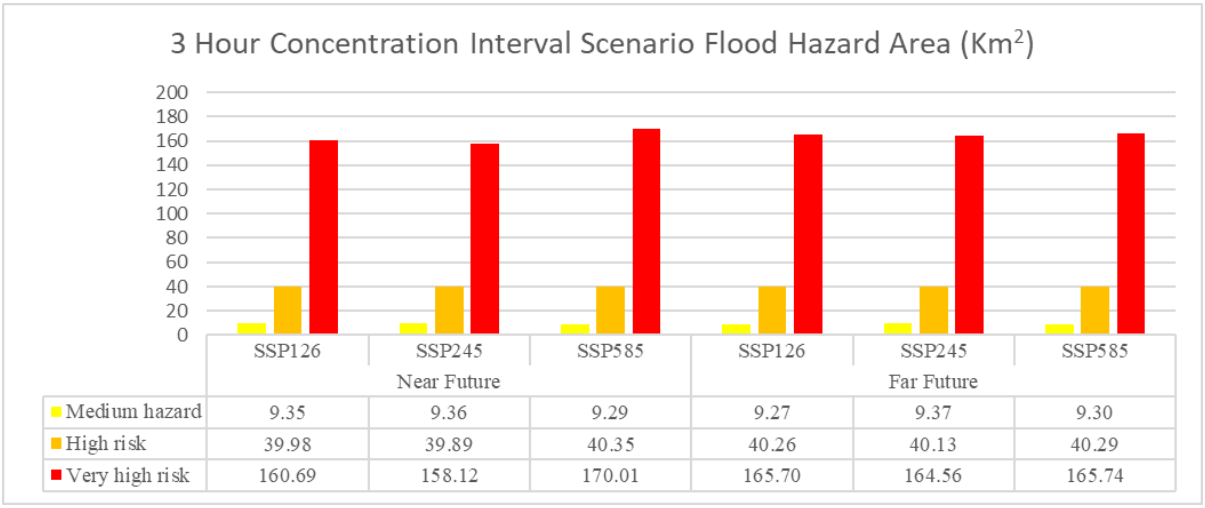

	SSP126	SSP245	SSP585	SSP126	SSP245	SSP585
	Near Future			Far Future		
Medium hazard	9.35	9.36	9.29	9.27	9.37	9.30
High risk	39.98	39.89	40.35	40.26	40.13	40.29
Very high risk	160.69	158.12	170.01	165.70	164.56	165.74

Figure 11. Graph showing comparison of the area in 3 hour's concentration of rainfall for each scenario.

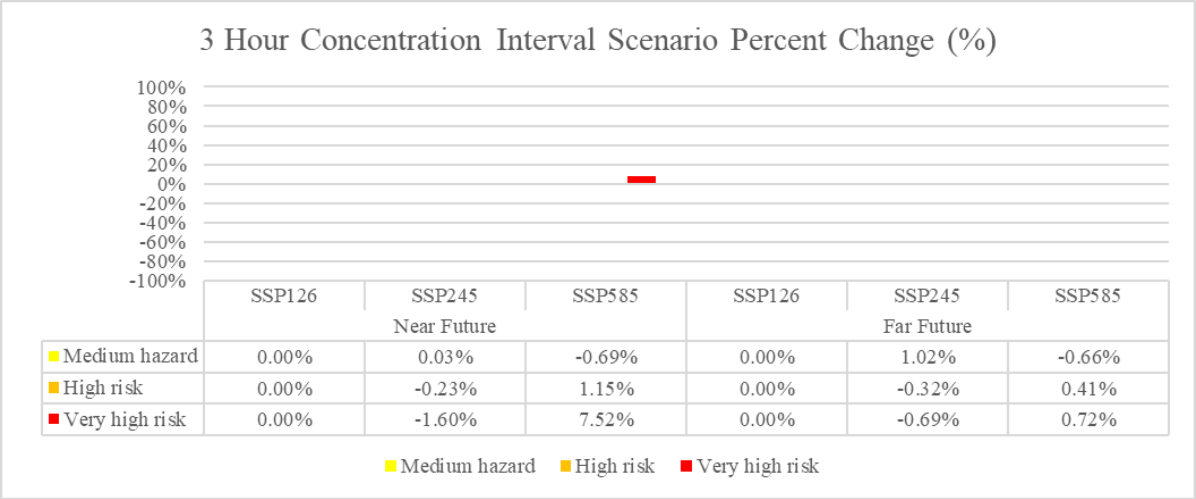

	SSP126	SSP245	SSP585	SSP126	SSP245	SSP585
	Near Future			Far Future		
Medium hazard	0.00%	0.03%	-0.69%	0.00%	1.02%	-0.66%
High risk	0.00%	-0.23%	1.15%	0.00%	-0.32%	0.41%
Very high risk	0.00%	-1.60%	7.52%	0.00%	-0.69%	0.72%

Figure 12. Graph showing the percent change in area in 3 hour's concentration of rainfall for each scenario.

6 Hour concentration interval

In the near future, the area prone to very high-risk flooding under the SSP-126 scenario is 144.35 km^2, the SSP-245 scenario has an area of 142.56 km^2, a decreased from the SSP-126 scenario of -1.24%, and the SSP585 scenario has an area of 151.16 km^2, an increased from the scenario in SSP-245 by 6.03%. According to the analysis, the scenario at SSP-585 was the worst-case scenario.

In the far future, the area prone to very high-risk flooding under the SSP-126 scenario is 148.81 km^2, the SSP-245 scenario has an area of 147.77 km^2, a decreased from the SSP-126 scenario of -0.70%, and the SSP585 scenario has an area of 148.99 km^2, an increased from the scenario in SSP-245 by 0.83%. According to the analysis, the scenario at SSP-585 was the worst-case scenario.

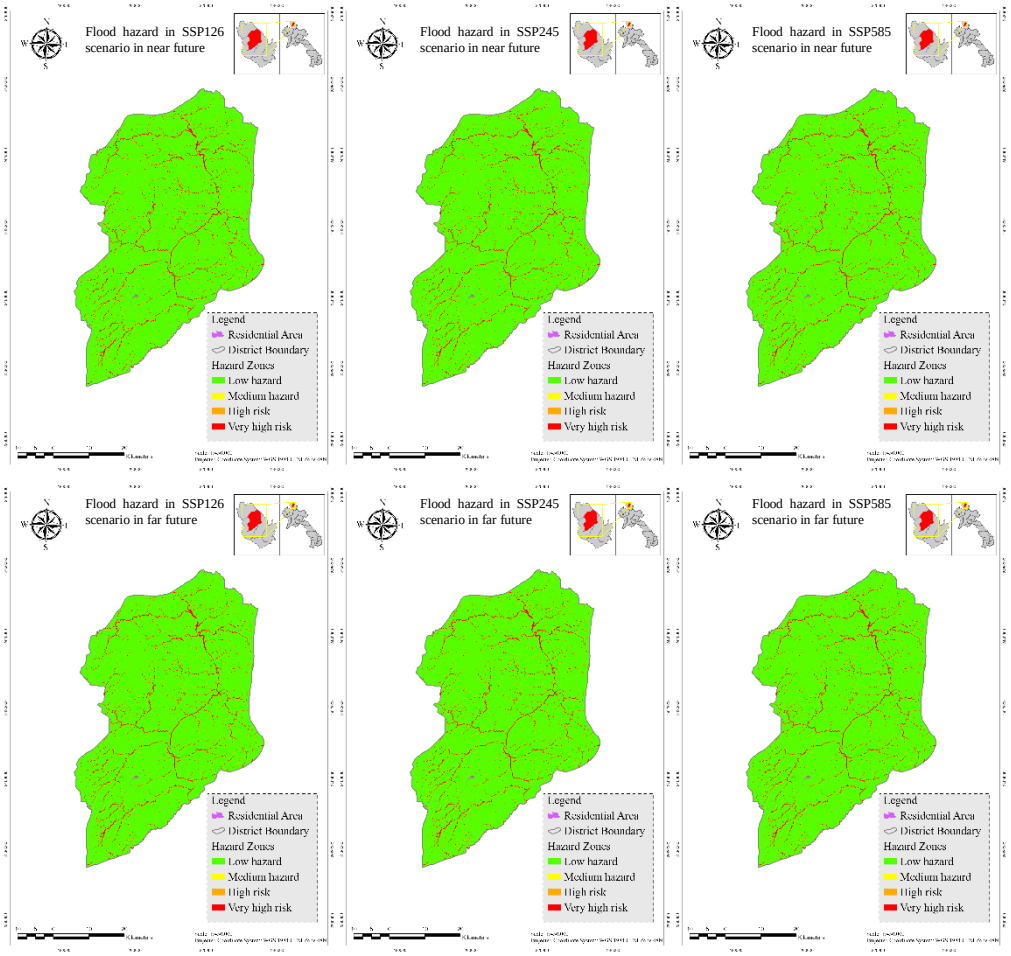

Figure 13. Flood hazard map in 6 hour's concentration of rainfall for each scenario.

Table 9. Flood hazard area in 6 hour's concentration of rainfall for each scenario.

6 Hours Concentration Interval Flood Hazard Area (km^2)							
No	**Hazard Zones**	**Near Future**			**Far Future**		
		SSP126	**SSP245**	**SSP585**	**SSP126**	**SSP245**	**SSP585**
1	Low hazard	2660.64	2662.51	2653.56	2656.20	2657.23	2659.28
2	Medium hazard	8.84	8.87	8.94	8.79	8.80	8.82
3	High risk	37.02	36.90	37.18	37.05	37.04	37.35
4	Very high risk	144.35	142.56	151.16	148.81	147.77	148.99

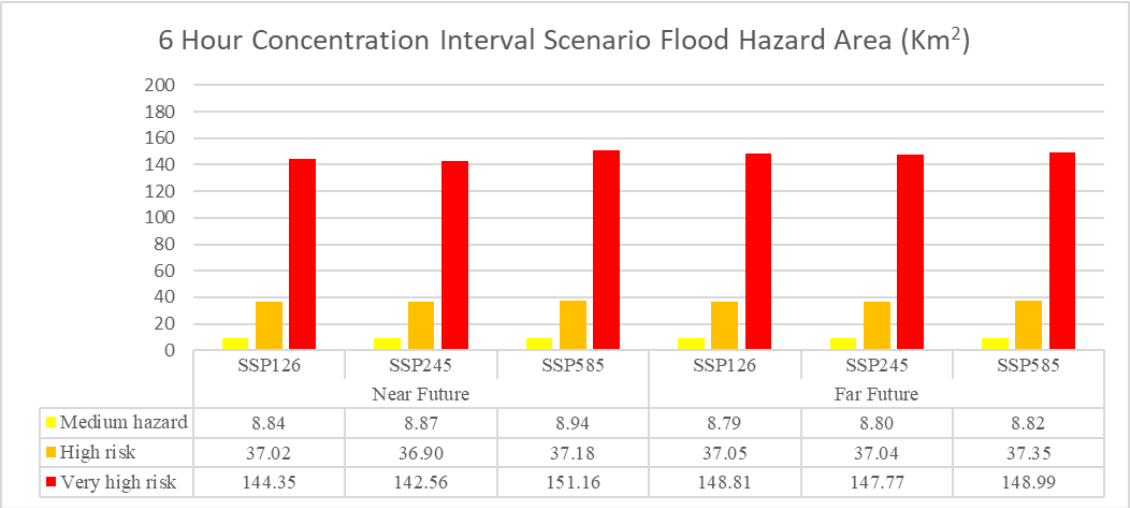

	SSP126	SSP245	SSP585	SSP126	SSP245	SSP585
	Near Future			Far Future		
Medium hazard	8.84	8.87	8.94	8.79	8.80	8.82
High risk	37.02	36.90	37.18	37.05	37.04	37.35
Very high risk	144.35	142.56	151.16	148.81	147.77	148.99

Figure 14. Graph showing comparison of the area in 6 hour's concentration of rainfall for each scenario.

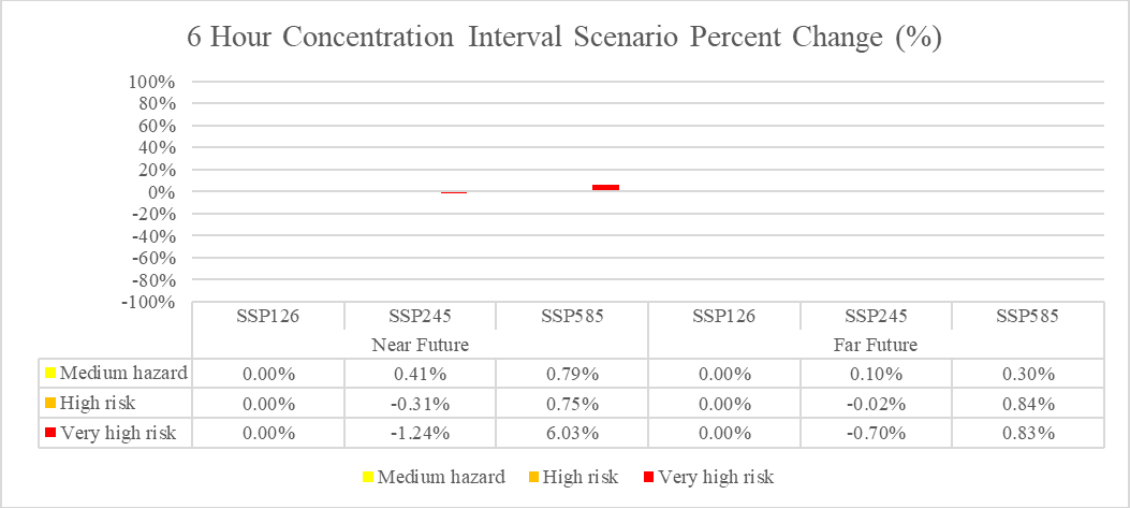

	SSP126	SSP245	SSP585	SSP126	SSP245	SSP585
	Near Future			Far Future		
Medium hazard	0.00%	0.41%	0.79%	0.00%	0.10%	0.30%
High risk	0.00%	-0.31%	0.75%	0.00%	-0.02%	0.84%
Very high risk	0.00%	-1.24%	6.03%	0.00%	-0.70%	0.83%

Figure 15. Graph showing the percent change in area in 6 hour's concentration of rainfall for each scenario.

Drought indices

In the near future, SPI_1 under SSP-126 experienced 16 droughts, SSP-245 experienced 19 of them, and SSP-585 experienced 19 of them. SPI_3 under SSP-126 experienced 10 droughts, and SSP-245 experienced 7, and SSP-585 appeared 17 times of them. In SPI_6 no drought was identified in any of the scenarios. Depending on how serious the scenario is, droughts happen more frequently.

(a)

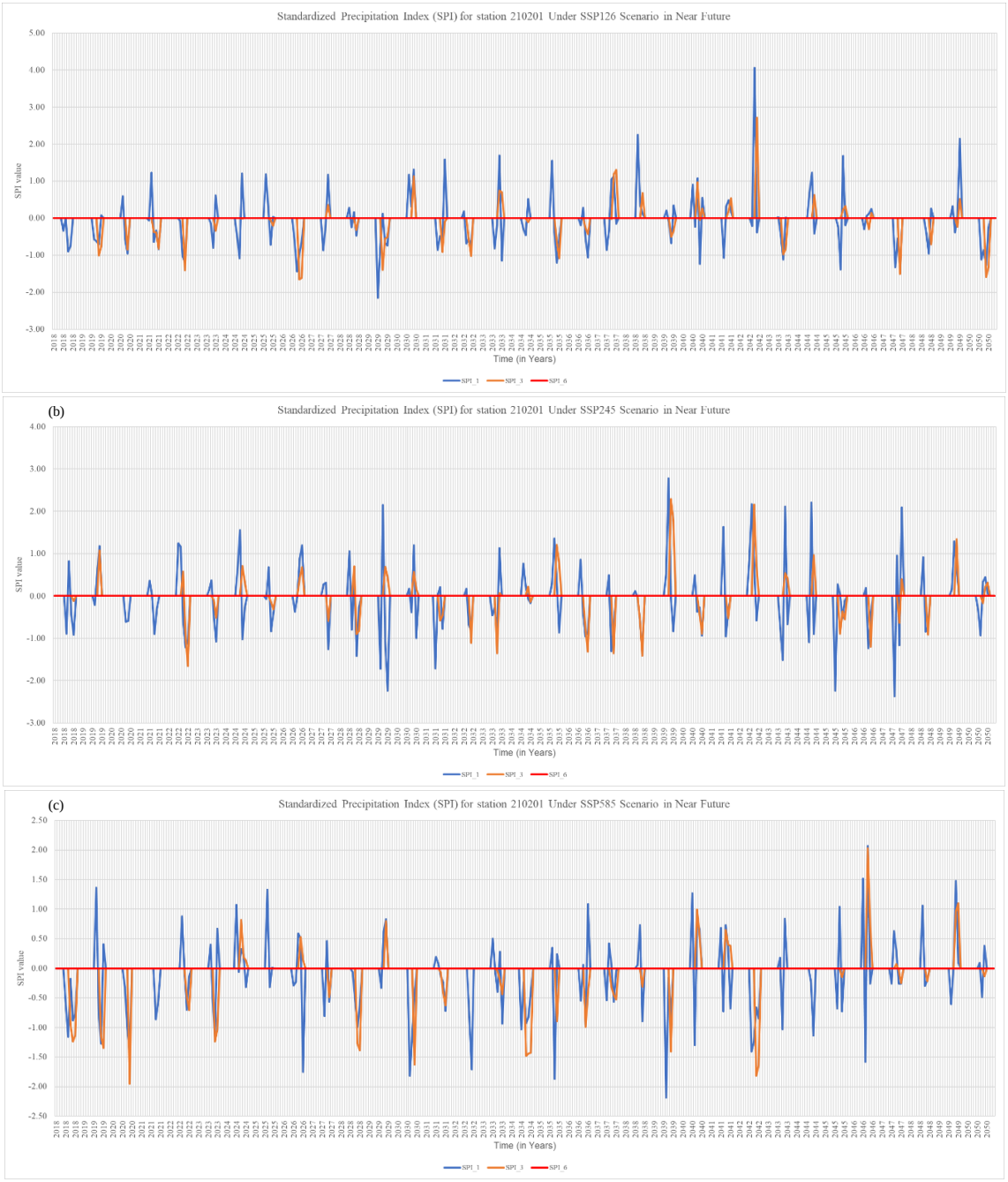

Figure 16. Comparison of SPI_1, SPI_3 and SPI_6 under (a) SSP-126, (b) SSP-245 and (c) SSP-585 in near future from year 2018-2050 at station 210201.

Table 10. Summary statistics of indices in near future.

Drought Index	**SSP-126**			**SSP-245**			**SSP-585**		
	SPI_1	**SPI_3**	**SPI_6**	**SPI_1**	**SPI_3**	**SPI_6**	**SPI_1**	**SPI_3**	**SPI_6**
Highest drought index	4.06	2.71	0.00	2.78	2.29	0.00	2.07	2.03	0.00
Lowest drought index	-2.15	-1.65	0.00	-2.37	-1.65	0.00	-2.19	-1.95	0.00
Total amont of drought (<-1, year)	16	10	0	19	7	0	19	17	0

In the far future, SPI_1 under SSP-126 experienced 32 droughts, SSP-245 experienced 29, and SSP-585 experienced 26 of them. SPI_3 under SSP-126 experienced 13 droughts, SSP-245 experienced 18, and SSP-585 appeared 7 times of them. In SPI_6 no drought was identified in any of the scenarios. In extreme scenarios, droughts occur less frequently.

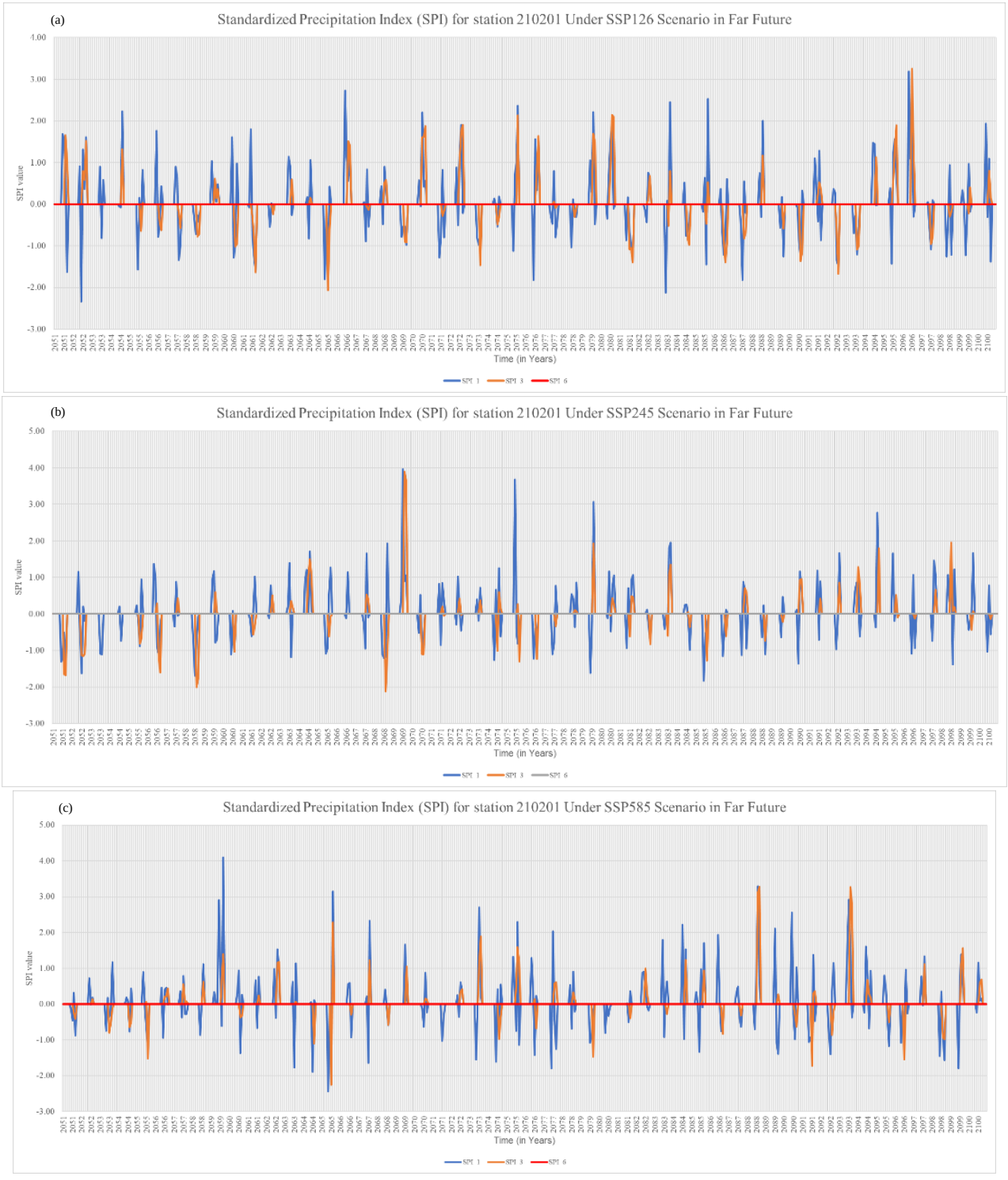

Figure 17. Comparison of SPI_1, SPI_3 and SPI_6 under (a) SSP-126, (b) SSP-245 and (c) SSP-585 in far future from year 2051-2100 at station 210201.

Table 11. Summary statistics of indices in far future.

Drought Index	SSP-126			SSP-245			SSP-585		
	SPI_1	**SPI_3**	**SPI_6**	**SPI_1**	**SPI_3**	**SPI_6**	**SPI_1**	**SPI_3**	**SPI_6**
Highest drought index	3.18	3.25	0.00	3.96	3.90	0.00	4.10	3.28	0.00
Lowest drought index	-2.33	-2.06	0.00	-1.83	-2.11	0.00	-2.44	-2.25	0.00
Total amount of drought (<-1, year)	32	13	0	29	18	0	26	7	0

Conclusion

Among other natural disasters, drought and flooding are undoubtedly among the more destructive yet little predicted ones. Using drought indicators for drought monitoring is frequently a crucial foundation. A better outlook of the potential risk that can befall the region is provided by drought indices and rainfall runoff models calculated from predicted rainfall. In this paper, a method is offered to compare rainfall concentration and drought indices at various time scales for further research into the respective.

Drought and flood are obviously one of the more damaging yet hardly determined natural disasters among others. Drought monitoring using drought indices often serves as an important base. Drought indices computed from forecasted rainfall gives a better outlook of potential risk that may be inflicted upon the region. In this study, a means is provided to compare among drought indices of different time scales for further study into respective drought types.

Floods are likely to become more severe as the scenario worsens. From the results of this analysis, in both periods of the 1-hour rainfall concentration under the SSP-585 scenario, there will be areas with the highest risk of flooding. In the near future, the frequency of droughts will increase as the scenario worsens, but in the far future, it will be the opposite. The frequency of droughts decreases as the scenario worsens.

Acknowledgement

The authors would like to acknowledge GEF, UNEP program for being very kind financial support which enabled us to gather relevant data for this study.

Funding: None

Conflict: The authors declare no conflict of interest

References

ADB. (2012). Greater Mekong Subregion Flood and Drought Risk Management and Mitigation Project (RRP REG 40190). Asian Developmet Bank.

Ashok K. Mishra, V. P. (2010). A review of drought concepts. Journal of Hydrology, 391(1-2), 202-216. doi:10.1016/j.jhydrol.2010.07.012

Changshen Cai, L. P.-J. (2015). Precise point positioning with quad-constellation: GPS, BeiDou, GLONASS and Galileo. Advances in Space Research, 56(1), 133-143. doi:10.1016/j.asr.2015.04.001

Christian Birkel, A. C. (2019). Rainfall-Rumoff Modeling: A Brief OVerview. Reference Module in Earth Systems and Environmental Sciences. doi:10.1016/B978-0-12-409548-9.11595-7

Claudia Teutschbein, J. S. (2012). Bias correction of regional climate model simulations for hydrological climate change impact studies: Review and evalation of different methods. Journal of Hydrology, 456-457, 12-19. doi:10.1016/j.jhydrol.2012.05.052

David wells, N. B.-P. (1999). Guide to GPS positioning. New Brunswick: Canada: University of New Brunswick Graphic Services.

Detlef P. van Vuuren, E. S. (2017). Energy, land-use and greenhouse gas eissions trajectories under a green growth paradigm. Global Environmental Change, 42, 237-250. doi:10.1016/j.gloenvcha.2016.05.008

Donald A. Wilthite, M. H. (1985). Understanding the Drought Phenomenon: The Role of Definitions. Water International, 10(3), 111-120. doi:10.1080/02508068508686328

Eden, U. (2012). Drought assessment by evapotranspiration mapping in Twente, The Netherlands. Enschede: Faculty of Geo-

Informatic Science and Earth Observation of the University of Twente.

Elmar Kriegler, N. B. (2017). Fossil-fueled development (SSP5): An engergy and resource intensive scenario for the 21st century. Global Environmental Change, 42, 297-315. doi:10.1016/j.gloenvcha.2016.05.015

GCF. (2021). Lao PDR Green Climate Fund Country Programme. Green Climate Fund.

Harald Kling, M. F. (2012). Runoff conditions in the upper Danube basin under an ensemble of climate change scenarios. Journal of Hydrology, 424-425, 264-277. doi:10.1016/j.jhydrol.2012.01.011

Hendricks, E. L. (1962). An understanding of water in relation to earth processes requires the collaboration of many disciplines. Hydrology, 135(3505), 699-705. doi:10.1126/science.135.3505.69

Hoshin V. Gupta, H. K. (2009). Decomposition of the mean squarred error and NSE performance criteria: Implication for imporoving hydrological modelling. Journal of Hydrology, 377(1-2), 80-91. doi:10.1016/j.jhydrol.2009.08.003

Hui Wan, X. Z. (2005). Stochastic modelling of daily precipitation for Canada. Atmosphere-Ocean, 43(1), 23-32. doi:10.3137/ao.430102

IFC. (2017). Nam Ou River Basin Profile. International Finance Coporation.

IPCC. (2013). Evaluation of Climate Models. In AR5 CLIMATE CHANGE 2013: THE PHYSICAL SCIENCE BASIS (pp. 741-866).

IPCC. (2014). AR5 Synthesis Report: Climate Change 2014. Intergovernmental Panel on Climate Change.

IPCC. (2021). Climate Change 2021: The Physical Science Basis, the Working Group I contribution to the Sixth Assessment Report. The Intergovernmental Panel on Climate Change.

J.E. Nash, J. S. (1970). River flow forecasting through conceptual models part I - Adiscussion of principles. Journal of Hydrology, 10(3), 282-290. doi:10.1016/0022-1694(70)90255-6

Jesslyn F. Brown, B. D. (2008). The Vegetation Drought Response Index (VegDRI): A New Integrated Approach for Monitoring Drought Stress in Vegetation. GIScience & Remote Sensing, 45(1), 16-46. doi:10.2747/1548-1603.45.1.16

Katherine Calvinm, B. B.-L. (2017). The SSP4: A world of deepening inequality. Global Environmental Change, 42, 284-296. doi:10.1016/j.gloenvcha.2016.06.010

Keywan Riahi, D. P. (2017). The Shared Socioeconomic Pathways and their energy, land use, and greenhouse gas emissions implications: An overview. Global Environmental Change, 42, 153-168. doi:10.1016/j.gloenvcha.2016.05.009

Li, K. (2000). Drought Early Warning and Impact Assessment in China. In W. M. Organization, Early Warning System for Drought preparedness and Drought Management. Lisbon, Portugal: World Meteorological Organization.

Lóczy, D. (2010). Flood hazard in Hungary: a re-assessment. Central European Journal of Geosciences, 2, 537-547. doi:10.2478/v10085-010-0029-0

Maisor. (2022). Estimate of flood hazard area under climate change conditions CMIP5 and CMIP6 scenario in the XeChamphone catchment area, Savannakhet Province. Faculty of Engineering, National University of Laos.

McCloy, K. R. (2013). Resource Management Information Systems (2nd ed.). London: Taylors & Francis Group. doi:10.1201/b17305

MRC. (2019). Annual Hydrology Flood and Drought Report. Mekong River Commission.

Niemeyer, S. (2008). New drought indices. In Conference Proceedings: Lopez-Francos A, 267 - 274.

Oliver Fricko, P. H. (2017). The marker quantification of the Shared Socioeconomic Pathway 2: A middle of the road scenario for the 21st century. Global Environmental Change, 42, 251-267. doi:10.1016/j.gloenvcha.2016.06.004

Parker, D. J. (2000). Flash floods. In E. &. Grundfest, Floods (Hazards & Disasters) (1st ed., Vol. I, pp. 377-390). Taylor & Francis Group. doi:10.4324/9781315830889

Phrakonkham, S. (2020). Integrated hazard and risk maps using Analytical Hierarchy Process considering land use and climate change issues in Lao PDR.

Rasanark, S. (2021). Study on the Impact of Climate Change on the Hydrology of Xedone river catchment area. Faculty of Engineering, National University of Laos.

Sally J. Priest, S. T.-R. (2009). Building Models to Estimate Loss of Life for Flood Events. FloodSite.

Shinichiro Fujimori, T. H. (2017). SSP3: AIM impplementation of Shared Socioeconomic Pathways. Global Environmental Change, 42, 268-283. doi:10.1016/j.gloenvcha.2016.06.009

Sickle, J. V. (2015). GPS for Land Surveyors (4th ed.). CRC Press.

Thomas B. McKee, N. J. (1993). The Relationship of Drought Frequency and Duration to Time Scales. In N. J. Thomas B. McKee, Eighth Conference on Applied Climatology (pp. 179-186). Anaheim, California: Department of Atmospheric Science Colorado State University Fort Collins.

UNDP. (2012). National Strategy on Climate Change of Lao PDR. United Nations Development Programme.

Wardlow, B. T. (2008). The Vegetation Drought Response Index (VegDRI): a new drought monitoring approach for vegetation. National Integrated Drought Information System (NIDIS) Knowledge Assessment Workshop-Contributions of Satellite Remote Sensing to Drought Monitoring, 6-7.

Weibull. (1939). A Statiscial Theory of the Strength of Materials.

Yangqing Lian, I.-C. C. (2007). Coupling of hydrologic and hydraulic models for the Illinois River Basin. Journal of Hydrology, 344(3-4), 210-222. doi:10.1016/j.jhydrol.2007.08.004

Yuk Feng Huang, J. T. (2016). Drought Forecasting using SPI and EDI under RCP-8.5 Cliamte Change Scenarios for Langat River Basin, Malaysia. Procedia Engineering, 154, 710-717. doi:10.1016/j.proeng.2016.07.573

Zeke hausfather, G. P. (2020). Emission-the'business as usual' story is misleading. Nature, 577, 618-620. doi:10.1038/d41586-020-00177-3